Catalysis Today 170 (2011) 76–84

Contents lists available at ScienceDirect

Catalysis Today

journal homepage: www.elsevier.com/locate/cattod

Zeolite framework stabilized nickel(0) nanoparticles: Active and long-lived catalyst for hydrogen generation from the hydrolysis of ammonia-borane and sodium borohydride

Mehmet Zahmakıran[1], Tuğçe Ayvalı, Serdar Akbayrak, Salim Çalışkan, Derya Çelik, Saim Özkar*

Department of Chemistry, Middle East Technical University, 06531 Ankara, Turkey

ARTICLE INFO

Article history:
Available online 22 October 2010

Keywords:
Zeolite
Nickel
Hydrolysis
Sodium borohydride
Ammonia borane
Hydrogen generation

ABSTRACT

Among the hydrogen storage materials, ammonia-borane and sodium borohydride appear to be promising candidates as they can release hydrogen on hydrolysis in aqueous solution under mild conditions. Here, we report the development of a cost-effective and highly active nickel(0) nanoparticles catalyst for the hydrolysis of ammonia-borane and sodium borohydride. Nickel(0) nanoparticles confined in zeolite framework were prepared by using our previously established procedure and characterized by ICP-OES, XRD, TEM, HR-TEM, SEM, EDX, XPS, Raman spectroscopy and N_2 adsorption–desorption technique. All the results show that nickel(0) nanoparticles are formed within the framework of zeolite-Y. Nickel(0) nanoparticles confined in zeolite framework are highly active catalyst in the hydrolytic dehydrogenations of sodium borohydride and ammonia-borane. This catalyst is isolable, bottleable, redispersible and reusable. The report also includes the detailed kinetic study of the catalytic hydrolysis of both substrates, ammonia-borane and sodium borohydride depending on the catalyst concentration, substrate concentration, and temperature.

1. Introduction

There has been rapidly growing interest for suitable hydrogen storage materials because the efficient storage of hydrogen is still one of the key issues in 'Hydrogen Economy', which would facilitate the transition from fossil fuels (i.e., petroleum, natural gas, and coal) to the renewable energy sources, on the way towards a sustainable energy future [1–4]. In this respect various solid materials, such as metal nitrides and imides [5], carbon nanotubes [6], TiO_2 nanotubes [7], zeolites [8], organic-polymers [9], metal-organic frameworks [10] and CBN compounds [11] have been considered for hydrogen storage. Additionally, in recent studies, boron based compounds including sodium borohydride ($NaBH_4$) [12], ammonia-borane (NH_3BH_3) [13], dimethylamine-borane ($(CH_3)_2HNBH_3$) [14] and ammonia-triborane ($H_3NB_3H_7$) [15] have also been considered to be used in chemical hydrogen storage [16]. Among these boron based materials sodium borohydride and ammonia borane seem to be promising candidates because of their low molecular weight and high hydrogen density [17,18]. The hydrogen gas can be generated from the catalytic hydrolysis of sodium borohydride (Eq. (1)) and ammonia-borane (Eq. (2)) under mild conditions [17]

$$NaBH_4 + 2H_2O \xrightarrow{\text{catalyst}} NaBO_2 + 4H_2 \quad (1)$$

$$H_3NBH_3 + 2H_2O \xrightarrow{\text{catalyst}} NH_4BO_2 + 3H_2 \quad (2)$$

Despite the difficulty in recycling the hydrolysis product metaborate anion, still one of the biggest impediments for potential applications, the hydrogen generation from the hydrolysis of sodium borohydride and ammonia-borane have some features which make them promising in potential applications; (i) $NaBH_4$ and H_3NBH_3 have high solubility in water (55.0 and 33.6 g/100 g water, respectively) [19], (ii) the hydrolysis reactions occur at appreciable rate only in the presence of a suitable catalyst at room temperature [20,21], (iii) both of these reactions are exothermic ($\Delta H^\circ = -155.97$ kJ/mol for H_3NBH_3 and -210 kJ/mol for $NaBH_4$) [22,23], (iv) the hydrolyses generate 4 and 3 equiv. of H_2 per mole of $NaBH_4$ and H_3NBH_3, respectively. Among the catalysts tested so far [24] noble metals such as Ru [25–28], Rh [28–31] and Pt [13,28,32] based catalysts have shown high activity in these hydrolysis reactions while their use in practical applications is restricted by their high material cost. On the other hand, the cheaper transition metal catalysts generally exhibit only low to moderate catalytic activity. However, recent advances in catalyst preparation technique have led to significant improvement in the catalytic activity of transi-

* Corresponding author. Tel.: +90 312 210 3212; fax: +90 312 210 3200.
E-mail address: sozkar@metu.edu.tr (S. Özkar).
[1] New address: Department of Chemistry, Van Yüzüncü, Yıl University, 65080 Van, Turkey.

0920-5861/$ – see front matter © 2010 Elsevier B.V. All rights reserved.
doi:10.1016/j.cattod.2010.09.022

tion metal catalysts, even to a level comparable to that of noble metal catalysts [33]. Indeed, recent studies [26] have shown that intrazeolite cobalt(0) [34], Ni/C [35], Ni/SiO_2 [36], MOF's [37] copper(0) nanoparticles [38] are highly active catalyst in the hydrolysis of sodium borohydride and ammonia borane, respectively. These results encouraged us to investigate the catalytic performances of zeolite framework stabilized non-noble metal(0) nanoparticles in these important reactions.

In this paper we report the preparation of nickel(0) nanoparticles confined in zeolite framework by using our previously established procedure [25,26,29–42] and their characterization by using ICP-OES, XRD, TEM, HR-TEM, SEM, EDX, XPS, Raman spectroscopy and N_2 adsorption–desorption technique. All the results reveal the formation of nickel(0) nanoparticles within the framework of zeolite-Y. The nickel(0) nanoparticles confined in zeolite framework were found to be active catalyst in the hydrolysis of both sodium borohydride and ammonia-borane even at low temperatures and low Ni loading. The reusability and catalytic lifetime experiments showed that nickel(0) nanoparticles confined in zeolite framework can be considered as an efficient, reusable and economical catalyst and may find applications in small scale hydrogen storage.

2. Experimental

2.1. Materials

Nickel(II) chloride hexahydrate ($NiCl_2{\cdot}6H_2O$), sodium zeolite-Y ($Na_{56}(AlO_2)_{66}(SiO_2)_{156}{\cdot}xH_2O$), sodium borohydride (98%), ammonia borane (97%), D_2O and $BF_3{\cdot}(C_2H_5)_2O$ were purchased from Aldrich. Deionized water was distilled by water purification system (Milli-Q System). All glassware and Teflon coated magnetic stir bars were cleaned with acetone, followed by copious rinsing with distilled water before drying in an oven at 150 °C.

2.2. Preparation of zeolite framework stabilized nickel(0) nanoparticles

Zeolite confined nickel(0) nanoparticles were prepared by following our previously established two step procedure [26,34,42]. Zeolite-Y was slurried with 0.1 M NaCl to remove sodium defect sites, washed until free of chloride and calcined in dry oxygen at 500 °C for 12 h before to use. Nickel(II) cations were introduced into the zeolite-Y by ion exchange [43] of 1000 mg Zeolite-Y in 100 mL aqueous solution of 100 mg $NiCl_2{\cdot}6H_2O$ for 72 h at room temperature. The sample was then filtered by suction filtration using Whatman-1 filter paper, washed three times with 20 mL of deionized water and the remnant was dried in vacuum. In the second step, the solid remnant was added into 100 mL $NaBH_4$ solution (250 mg, 6.6 mmol) at room temperature. Nickel(II) ion was reduced and the nickel(0) nanoparticles were formed; the reduction was considered to be complete when no more hydrogen evolution was observed. The zeolite framework stabilized nickel(0) nanoparticles sample was filtered again by suction filtration using Whatman-1 filter paper, washed three times with 20 mL of deionized water, and dried under N_2 gas purging at room temperature for 24 h, then transferred into the drybox (O_2 < 5 ppm, H_2O < 1 ppm).

2.3. Characterization of zeolite framework stabilized nickel(0) nanoparticles

The nickel contents of the zeolite samples were determined by Inductively Coupled Plasma Optical Emission Spectroscopy (ICP-OES, Leeman-Direct Reading Echelle) after each sample was completely dissolved in the mixture of HNO_3/HCl (1/3 ratio). Powder X-ray diffraction (XRD) patterns were recorded on a MAC Science MXP 3TZ diffractometer using Cu Kα radiation (wavelength 1.5406 Å, 40 kV, 55 mA). Transmission electron microscopy (TEM) was performed on a JEM-2010F microscope (JEOL) operating at 200 kV. A small amount of powder sample was placed on the copper grid of the transmission electron microscope. Samples were examined at magnification between 100 and 400K. Scanning electron microscope (SEM) images were taken using a JEOL JSM-5310LV at 15 kV and 33 Pa in a low-vacuum mode without metal coating on aluminum support. The elemental analysis was performed with an energy dispersive X-ray (EDX) analyzer (KEVEX Delta series) mounted on the Hitachi S-800. The nitrogen adsorption/desorption experiments were carried out at 77 K using a NOVA 3000 series (Quantachrome Instruments) instrument. The sample was outgassed under vacuum at 573 K for 3 h before the adsorption of nitrogen. The XPS analysis performed on a Physical Electronics 5800 spectrometer equipped with a hemispherical analyzer and using monochromatic Al Kα radiation (1486.6 eV, the X-ray tube working at 15 kV, 350 W and pass energy of 23.5 keV). ^{11}B NMR spectra were recorded on a Bruker Avance DPX 400 with an operating frequency of 128.15 MHz for ^{11}B. D_2O and $BF_3{\cdot}(C_2H_5)_2O$ were used as a lock and an external reference, respectively. At the end of the hydrolysis reaction, the resulting solutions were filtered and the filtrates were collected for ^{11}B NMR analysis.

2.4. Method for testing the catalytic activity of zeolite framework stabilized nickel(0) nanoparticles in the hydrolysis of sodium borohydride and ammonia borane

The catalytic activity of nickel(0) nanoparticles in the hydrolysis of sodium borohydride and ammonia-borane were determined by measuring the rate of hydrogen generation [44]. To determine the rate of hydrogen generation the catalytic hydrolysis of sodium borohydride or ammonia-borane was performed using a Fischer–Porter (FP) pressure bottle. The FP bottle was connected to a line through Swagelock TFE-sealed quick connects and to an Omega PX-302 pressure transducer interfaced through an Omega D1131 digital transmitter to a computer using the RS-232 module. The progress of an individual hydrolysis reaction was followed by monitoring the increase in the pressure of H_2 gas on Lab View 8.0 program. The pressure vs. time data was processed using Microsoft Office Excel 2003 and Origin 7.0 then converted into the values in proper unit, volume of hydrogen (mL). In a typical experiment, the desired amount of substrate was dissolved in 10 mL water. This solution was transferred with a glass-pipette into the FP bottle thermostated at 25.0 ± 0.1 °C. Then, zeolite framework stabilized nickel(0) nanoparticles sample was added into this solution. The experiment was started by closing the FP bottle connected to the pressure transducer and turning on the stirring at 1000 rpm simultaneously. In addition to the volumetric measurement of the hydrogen evolution, the conversion of sodium borohydride (δ = −42.1) [45] and ammonia-borane (δ = −24 ppm) [31] to borate (δ = 9–18 ppm) [31,45] was also checked by ^{11}B NMR spectroscopy.

2.5. Effect of nickel loading on the catalytic activity of zeolite framework stabilized nickel(0) nanoparticles

In a series of experiments the catalytic activity of zeolite framework stabilized nickel(0) nanoparticles ([Ni] = 1 mM) with a various nickel loading, wt% Ni (0.4, 0.6, 1.9, 2.4, 3.8) were tested in the hydrolysis of 10 mL of 100 mM $NaBH_4$ solution at 25 ± 0.1 °C. The experiments were performed in the same way as described in Section 2.4. The best catalytic activity was achieved by 0.6% nickel loaded catalyst. For all the tests reported hereafter, the nickel loading used was ∼0.6 wt% unless otherwise stated.

2.6. Zeolite catalyzed hydrolysis of sodium borohydride and ammonia-borane

To investigate the effect of the host material zeolite-Y on the catalytic activity of zeolite framework stabilized nickel(0) nanoparticles, the hydrolysis of sodium borohydride or ammonia-borane (100 mM in 10 mL) were performed in the presence of 800 mg zeolite-Y, corresponding to maximum amount of zeolite-Y used as a host material for all the tests reported here, at 25 ± 0.1 °C. The same experiments were repeated at different temperatures (20, 30, 35, 40 and 45 °C).

2.7. Kinetic study of the hydrolysis of sodium borohydride and ammonia-borane catalyzed by zeolite framework stabilized nickel(0) nanoparticles

In order to establish the rate laws for catalytic hydrolysis of sodium borohydride and ammonia-borane using zeolite framework stabilized nickel(0) nanoparticles (with 0.6 wt% nickel loading), for each substrate two different sets of experiments were performed in the same way as described in Section 2.4. In the first set of experiments, the concentration of substrate was kept constant at 100 mM (in 10 mL) and the nickel concentration was varied in the range of 1.0, 2.0, 3.0, 4.0 and 8.0 mM. In the second set of experiments, nickel concentration was held constant at 4.0 mM (in 10 mL) while the substrates concentrations were varied in the range of 50, 100, 200, 300 and 400 mM. Finally, we performed the catalytic hydrolysis of sodium borohydride and ammonia-borane in the presence of zeolite framework stabilized nickel(0) nanoparticles at constant substrate (100 mM in 10 mL) and nickel (4.0 mM in 10 mL) concentrations at various temperatures in the range of 20–40 °C in order to obtain the activation energy (E_a).

2.8. Isolability and reusability of zeolite framework stabilized nickel(0) nanoparticles catalyst in the hydrolysis of sodium borohydride and ammonia-borane

After the first run of hydrolysis of 100 mM substrate (in 10 mL), catalyzed by 4 mM nickel(0) nanoparticles at 25 ± 0.1 °C, the catalyst was isolated by suction filtration, washed three times with 20 mL of deionized water, and dried under N_2 gas purging at room temperature then transferred into the glove box. The dried samples of nickel(0) nanoparticles were weighted (there is no catalyst loss in repeating steps) and used again in the hydrolysis of 100 mM substrate and the same procedure was repeated three times. The results were expressed as percentage of initial catalytic activity zeolite framework stabilized nickel(0) nanoparticles and conversion in the hydrolysis of sodium borohydride and ammonia-borane.

2.9. Determination of the catalytic lifetime of zeolite framework stabilized nickel(0) nanoparticles catalyst in the hydrolysis of sodium borohydride and ammonia-borane

The catalytic lifetime of zeolite framework stabilized nickel(0) nanoparticles in the hydrolysis of sodium borohydride and ammonia-borane were determined by measuring the total turnover number (TTO). This experiment was started with a 15 mL solution containing 0.5 mM zeolite framework stabilized nickel(0) nanoparticles and 1.33 M substrate at 25.0 ± 0.1 °C. When the complete conversion is achieved, more substrate was added into the solution and the reaction was continued in this way until hydrogen gas evolution was slowed down to the level obtained in the $Na_{56}Y$ catalyzed hydrolysis of sodium borohydride or ammonia borane at 25 °C.

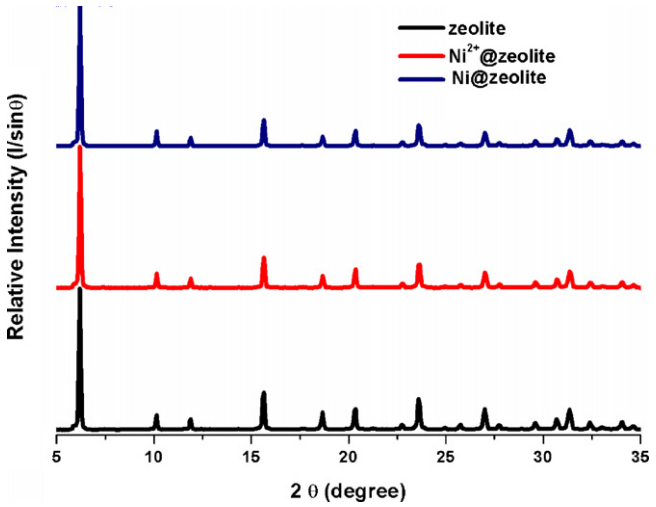

Fig. 1. The powder XRD patterns of zeolite-Y ($Na_{56}Y$), Ni^{2+}-exchanged zeolite-Y (Ni^{2+}@zeolite, with a rhodium loading of 0.6 wt%), zeolite framework stabilized nickel(0) nanoparticles Ni@zeolite prepared from the borohydride reduction of Ni^{2+}-exchanged zeolite-Y.

3. Results and discussions

3.1. Preparation and characterization of nickel(0) nanoparticles stabilized by zeolite framework (Ni@zeolite)

Zeolite framework stabilized nickel(0) nanoparticles, hereafter referred to as Ni@zeolite, were prepared by using our previously established procedure [26]; ion-exchange of Ni^{2+} ions with the extra framework Na^+ ions of zeolite-Y, followed by reduction of the Ni^{2+} ions in the framework of zeolite-Y with sodium borohydride in aqueous solution, all at room temperature. Following the procedure, first Ni^{2+}-exchanged zeolite-Y sample was obtained and characterized by XRD and ICP-OES. As seen from the comparison of XRD patterns of zeolite-Y and Ni^{2+}-exchanged zeolite-Y (Fig. 1), there is no noticeable change in both the intensities and positions of the Bragg peaks, indicating that neither the crystallinity nor the lattice of zeolite-Y is altered by the ion exchange. Next, the Ni^{2+}-exchanged zeolite-Y was reduced by sodium borohydride in aqueous solution yielding Ni@zeolite. Fig. 1 shows XRD patterns of Ni@zeolite, zeolite-Y and Ni^{2+}-exchanged zeolite-Y altogether and the comparison of them clearly shows that the incorporation of nickel(II) ion into zeolite and the reduction of nickel(II) ion forming the nickel(0) nanoparticles within the supercages cause no observable alteration in the framework lattice and no loss in the crystallinity of zeolite-Y.

The morphology and composition of Ni@zeolite were investigated by TEM, HRTEM, SEM, EDX and ICP-OES analyses. Fig. 2(a) shows SEM image of Ni@zeolite with a nickel loading of 2.4 wt% indicating that (i) there exist only crystals of zeolite-Y, (ii) there is no bulk nickel formed in observable size outside the zeolite crystals, (iii) the method used for the preparation of Ni@zeolite does not cause any observable defects in the structure of zeolite-Y, a fact which is also supported by the XRD results. The transmission electron microscopy (TEM) in Fig. 2(b and c) shows the presence of some nickel(0) nanoparticles of 3.9 ± 0.9 nm size on the external surface of zeolite. These nanoparticles appear to be stable and do not agglomerate to the bulk metal. TEM/EDX spectrum of Ni@zeolite given in Fig. 2(d) is showing that nickel is the only element detected in addition to the zeolite framework elements (Si, Al, O, Na) and Cu from the grid. The XRD, XPS, SEM, ICP-OES TEM and TEM-EDX analyses reveal that there is no bulk metal formation, only nickel(0) nanoparticles with an average size of 3.9 ± 0.9 nm size mostly on the external surface of zeolite.

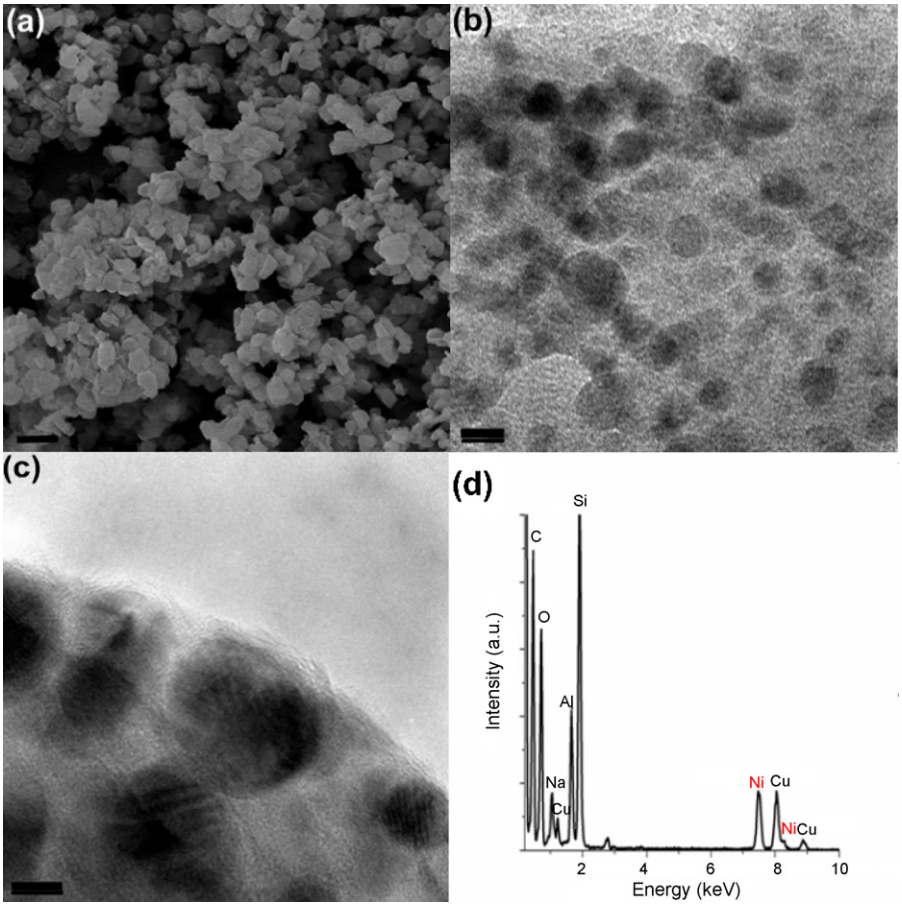

Fig. 2. (a) Scanning electron microcopy (SEM) image of Ni@zeolite (scale bar = 1 μm), (b) transmission electron microscopy (TEM) image of Ni@zeolite (scale bar = 10 nm), (c) TEM image of Ni@zeolite (scale bar = 5 nm), and (d) TEM modulated-energy dispersive X-ray spectrum (TEM-EDX) of Ni@zeolite.

Nitrogen adsorption–desorption isotherms of zeolite-Y and Ni@zeolite (2.4 wt% nickel) are given in Fig. 3 and both of them show Type I shape, a characteristic of microporous materials [46]. The micropore volume and area were determined for zeolite-Y and Ni@zeolite by *t*-plot method [47]. On passing from zeolite-Y to Ni@zeolite, both the micropore volume (from 0.443 to 0.218 cm^3/g) and the micropore area (from 816 to 527 m^2/g) are noticeably reduced. The remarkable decrease in the micropore volume and micropore area can be attributed to the encapsulation of nickel species in the cavities of zeolite-Y. Furthermore, no hysteresis loop was observed in the N_2 adsorption–desorption isotherm of Ni@zeolite indicating that the procedure followed in the preparation of Ni@zeolite does not create any mesopores.

XPS spectrum of the sample prepared by the reduction of Ni^{2+}-exchanged zeolite-Y with a nickel content of 2.4 wt% is given in Fig. 4. The peak fit of Ni 2p core level reveals four peaks at 856 eV for Ni(0) $2p_{3/2}$, 861 eV for Ni(II) $2p_{3/2}$, 873 eV for Ni(0) $2p_{1/2}$, 879 eV

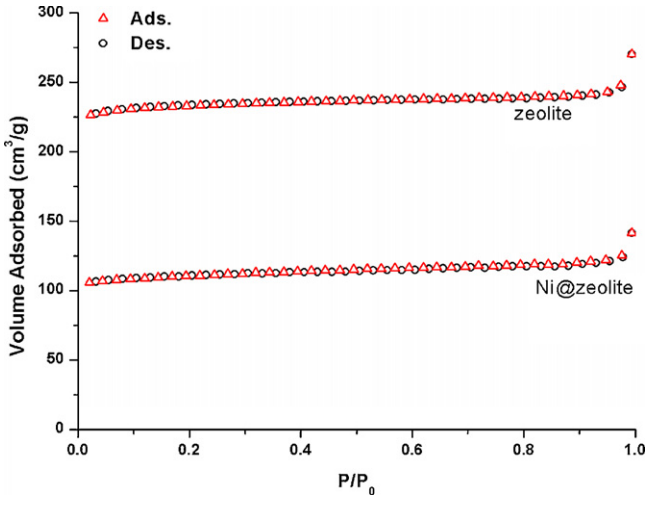

Fig. 3. The nitrogen adsorption–desorption isotherms of zeolite-Y and Ni@zeolite.

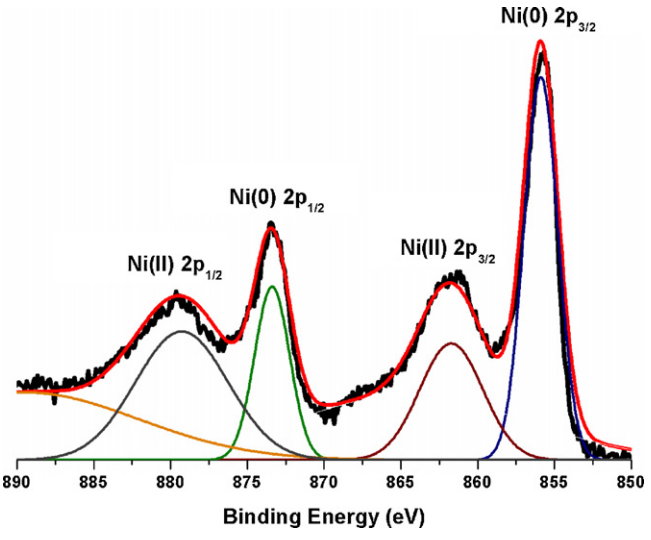

Fig. 4. High resolution Ni 3p XPS spectrum and its simulated peak fit of Ni@zeolite.

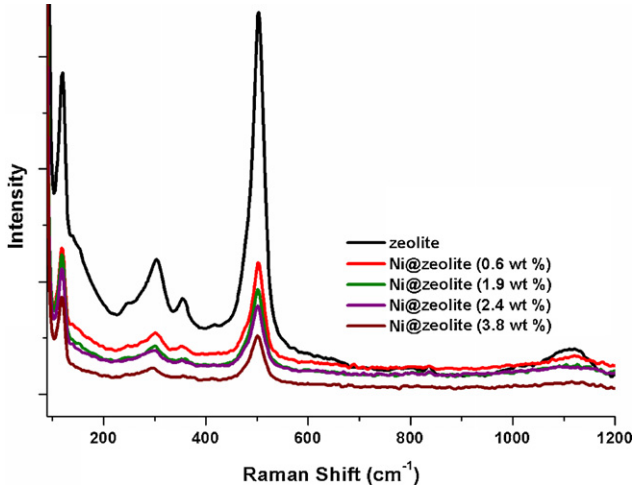

Fig. 5. Raman spectra of zeolite-Y and Ni@zeolite with various nickel loading (in wt%).

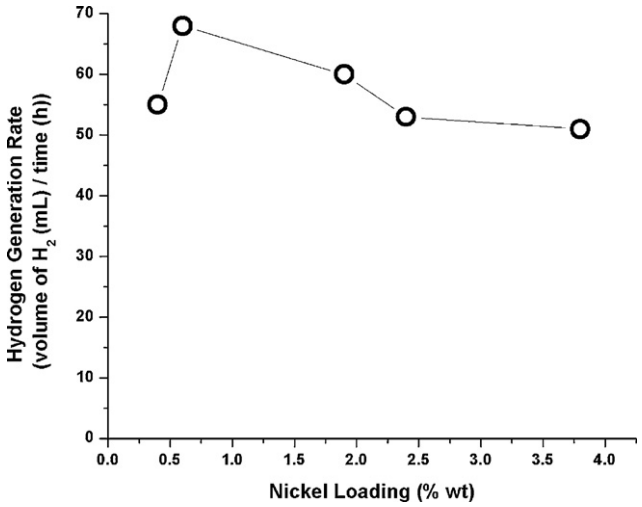

Fig. 6. The rate of hydrogen generation versus nickel loading (in wt%) for the hydrolysis of sodium borohydride (100 mM) catalyzed by zeolite-Y and Ni@zeolite with various nickel loading (1.0 mM Ni) at 25.0 ± 0.1 °C.

for Ni(II) $2p_{1/2}$. Compared to the values of nickel metal, 853 and 870 eV for the Ni(0) $2p_{3/2}$ and $2p_{1/2}$, respectively [48], the binding energies of Ni@zeolite are shifted by 3 eV toward higher values which might be attributed to both the quantum size effect [49] and peculiar electronic properties of the zeolite matrix [50,51]. The interaction of nickel(0) nanoparticles with the framework oxygen of the zeolite cages is expected to induce a positive charge on the surface metal which would increase the binding energies of nickel(0) nanoparticles. A similar effect has also been observed for the zeolite encapsulated cobalt [50] and platinum [52]. In addition to matrix effect, the high energy shift in the nickel binding energy might be due to the fact that electrons in the core level are strongly restricted by the atomic nucleus as observed in the case of palladium(0) nanoparticles in zeolite-Y [53].

Although oxidation of nickel(0) nanoparticles during the XPS sampling procedure is a well known phenomenon [50], the results obtained from XPS analysis need to be tested by using other analytical techniques. Raman spectroscopy was used to check whether nickel(II) oxide is really formed during the XPS sampling procedure or in the preparation of Ni@zeolite. Raman spectroscopy is a strong tool to test the existence of metal oxides [54]. Fig. 5 shows the Raman spectra of fresh samples of the host material zeolite-Y and Ni@zeolite prepared by borohydride reduction of Ni^{2+}-exchanged zeolite-Y. As it can be seen from Fig. 5, there is no noticeable difference between the spectra of Ni@zeolite (with different nickel loadings) and zeolite-Y. Thus, Raman spectroscopic analysis does not give any indication for the existence of NiO, while the XPS shows some oxide bands leading to the conclusion that the surface oxidation of nickel(0) nanoparticles occurs during the XPS sampling procedure.

3.2. Zeolite-Y catalyzed hydrolysis of sodium borohydride and ammonia-borane

Before testing the catalytic activity of Ni@zeolite in hydrogen generation from the hydrolysis of sodium borohydride and ammonia-borane, control experiments had to be performed:

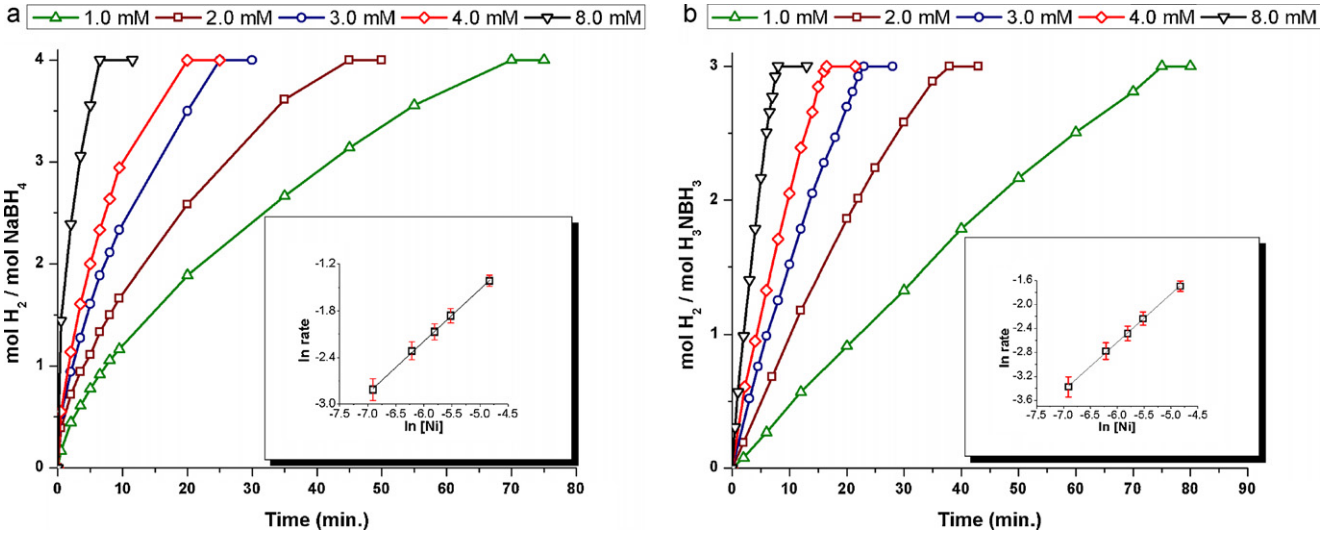

Fig. 7. (a) Plot of mole H_2/mole $NaBH_4$ versus time (min) for the hydrolysis of sodium borohydride ([$NaBH_4$] = 100 mM) catalyzed by Ni@zeolite with different nickel concentrations as given on the graph at 25.0 ± 0.1 °C. Inset: plot of the hydrogen generation rate versus the catalyst concentration (both in logarithmic scale) in the hydrolysis of $NaBH_4$ catalyzed by Ni@zeolite at 25.0 ± 0.1 °C ($y = 1.80 + 0.93x$). (b) Plot of mole H_2/mole H_3NBH_3 versus time (min) for the hydrolysis of ammonia-borane ([H_3NBH_3] = 100 mM) catalyzed by Ni@zeolite with different nickel concentrations as given on the graph at 25.0 ± 0.1 °C. Inset: plot of the hydrogen generation rate versus the catalyst concentration (both in logarithmic scale) in the hydrolysis of H_3NBH_3 catalyzed by Ni@zeolite at 25.0 ± 0.1 °C ($y = 1.83 + 0.97x$).

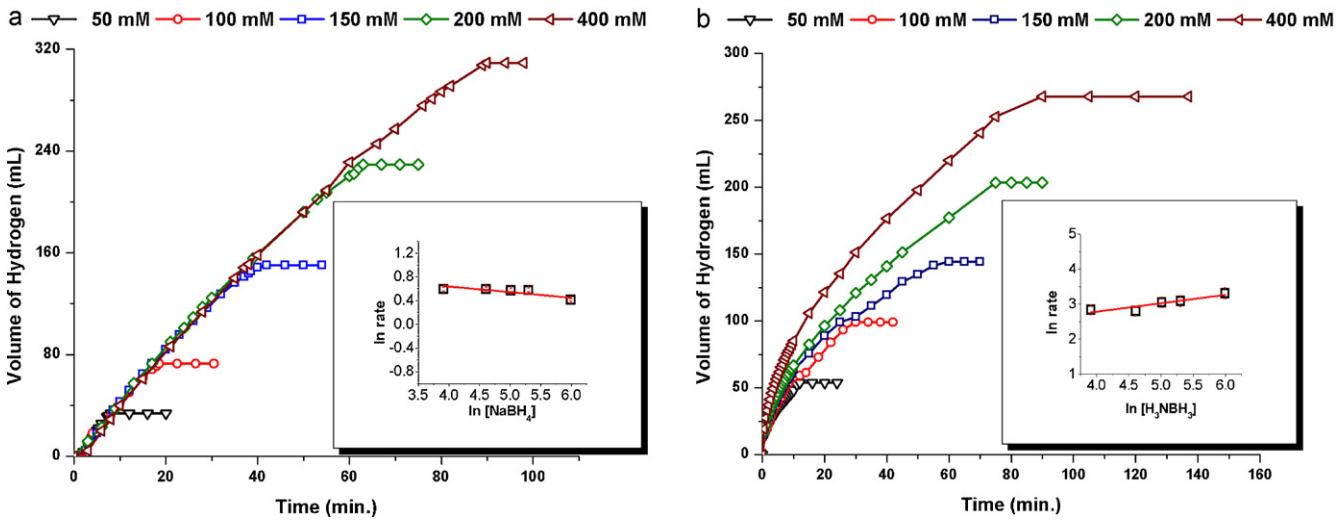

Fig. 8. (a) Plot of the volume of hydrogen (mL) versus time (s) for the hydrolysis of sodium borohydride catalyzed by Ni@zeolite ([Ni] = 4.0 mM) with different sodium borohydride concentrations as given on the graph at 25.0 ± 0.1 °C. Inset: Plot of the hydrogen generation rate versus sodium borohydride concentration (both in logarithmic scale) in the Ni@zeolite catalyzed hydrolysis of $NaBH_4$ at 25.0 ± 0.1 °C ($y = 0.02 - 0.09x$). (b) Plot of the volume of hydrogen (mL) versus time (s) for the hydrolysis of ammonia-borane catalyzed by Ni@zeolite ([Ni] = 4.0 mM) with different ammonia-borane concentrations as given on the graph at 25.0 ± 0.1 °C. Inset: Plot of the hydrogen generation rate versus ammonia-borane concentration (both in logarithmic scale) in the Ni@zeolite catalyzed hydrolysis of H_3NBH_3 at 25.0 ± 0.1 °C ($y = 1.82 + 0.19x$).

the hydrolysis of sodium borohydride and ammonia-borane in the presence of zeolite-Y to check whether zeolite-Y catalyzes the reactions. The experiment started with 10 mL solution of 100 mM sodium borohydride or ammonia-borane containing 8 wt% zeolite-Y gives 30 or 3.2 mL H_2 gas/h, respectively [55,56]. The hydrogen generation from the hydrolysis of sodium borohydride and ammonia-borane in the presence of zeolite-Y at an extremely slow rate is due to the Brønsted acid sites in the zeolite-Y [43]. That the Brønsted acid sites in zeolite catalyze the hydrolysis of ammonia-borane has already been shown by using H-type zeolites (H-BEA, H-MOR) as catalyst in the same reaction [32]. Although the hydrolyses of sodium borohydride and ammonia-borane in the presence of zeolite-Y are slow, all of the catalytic activity results of Ni@zeolite in the hydrolysis of sodium borohydride or ammonia-borane given here were corrected by subtracting the hydrogen gas generated from the hydrolysis of sodium borohydride or ammonia-borane in the presence of zeolite-Y under otherwise identical conditions.

3.3. Effect of nickel loading on the catalytic activity of Ni@zeolite

As the next, the hydrolysis of 100 mM $NaBH_4$ was performed by using Ni@zeolite sample with different nickel content in the range of 0.4–3.8 wt% to determine the effect of nickel loading on the catalytic activity of Ni@zeolite. The hydrogen generation rate in the catalytic hydrolysis of sodium borohydride was determined for hydrolysis of sodium borohydride catalyzed by Ni@zeolite containing 0.4–3.8 wt% Ni and used for the construction of Fig. 6. The variation in catalytic activity (Fig. 6) reflects the accessibility of nickel(0) nanoparticles in the zeolite framework by the substrate. The highest catalytic activity is obtained by using Ni@zeolite containing 0.6 wt% Ni, mostly on the surface and readily accessible. The small size of Ni@zeolite containing 0.6 wt% Ni may be another reason for its high activity. Although an informative TEM image of the 0.6 wt% Ni sample could not be obtained, this sample is expected to have smaller nickel(0) nanoclusters than the other samples containing higher nickel content. For all the other test

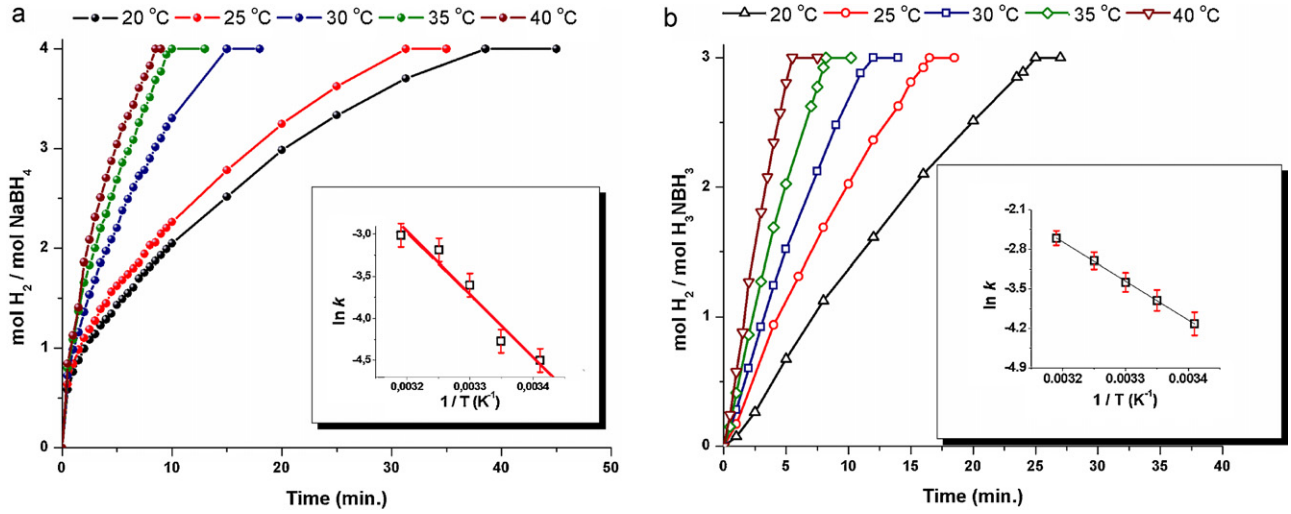

Fig. 9. (a) Plot of mole H_2/mole $NaBH_4$ versus time (min) for the hydrolysis of sodium borohydride ([$NaBH_4$] = 100 mM) catalyzed by Ni@zeolite [Ni] = 4 mM at different temperatures as given on the graph. Inset: Arrhenius plot for the Ni@zeolite catalyzed hydrolysis of sodium borohydride ($y = 20.65 - 7264x$). (b) Plot of mole H_2/mole H_3NBH_3 versus time (min) for the hydrolysis of sodium borohydride ([H_3NBH_3] = 100 mM) catalyzed by Ni@zeolite [Ni] = 4 mM at different temperatures as given on the graph. Inset: Arrhenius plot for the Ni@zeolite catalyzed hydrolysis of sodium borohydride ($y = 19.42 - 6543x$).

reactions performed in this study, samples of Ni@zeolite containing 0.6 wt% Ni were used.

3.4. Kinetics of Ni@zeolite catalyzed hydrolysis of sodium borohydride and ammonia-borane

The kinetics of both hydrolyses catalyzed by Ni@zeolite were studied depending on the catalyst concentration, substrate concentration, and temperature. Fig. 7 shows the plots of the stoichiometric ratio of H_2 generated to $NaBH_4$ or $H_3N{\cdot}BH_3$ versus time during the catalytic hydrolysis of 100 mM substrate solution in the presence of Ni@zeolite (with a nickel loading of 0.6 wt%) in different nickel concentration at $25.0 \pm 0.1\,^{\circ}C$. Almost a linear hydrogen generation starts immediately for the hydrolysis of both substrates as preformed catalyst is used, and continues until the complete consumption of substrate, though with a noticeable decrease in the rate toward the end. For example, using Ni@zeolite in 1.0 mM nickel concentration leads to a complete hydrogen release in the hydrolysis of sodium borohydride and ammonia-borane with *initial* turnover frequencies [57] of 950 and 305 h^{-1} at $25.0 \pm 0.1\,^{\circ}C$. Plotting the hydrogen generation rate, determined from the linear portion of each plot in Fig. 7, versus nickel concentration, both in logarithmic scales (insets in Fig. 7a and b), gives straight lines with a slope of 0.93 or 0.97, respectively, indicating that the hydrolytic dehydrogenation of sodium borohydride and ammonia-borane are first order with respect to the nickel concentration.

The effect of substrate concentration on the hydrogen generation rate was also studied by performing a series of experiments starting with varying initial concentration of substrate while keeping the catalyst concentration constant at [Ni] = 4.0 mM. Fig. 8 shows the plot of H_2 volume generated versus time for various initial concentrations of sodium borohydride and ammonia-borane and the plot of H_2 generation rate versus substrate concentration both on logarithmic scales in the insets. The results show that the catalytic hydrolysis of both sodium borohydride and ammonia-borane are proceeding in zero order with respect to substrate concentration. Taking all the results together reveals that the hydrolysis reaction of both substrates, sodium borohydride and ammonia-borane, is first order.

3.5. Effect of temperature and determination of the activation energies for the Ni@zeolite catalyzed hydrolysis of sodium borohydride and ammonia-borane

Ni@zeolite catalyze the hydrolytic dehydrogenations of sodium borohydride and ammonia-borane even at low temperatures. Fig. 9 shows the plots of the stoichiometric ratio of H_2 generated to $NaBH_4$ or H_3NBH_3 versus time for the Ni@zeolite catalyzed hydrolysis of sodium borohydride and ammonia-borane, respectively at various temperatures. The rates of hydrogen generation from the hydrolytic dehydrogenations of sodium borohydride and ammonia-borane in the presence of Ni@zeolite were measured from the linear portion of each plot given in Fig. 9(a) and (b) at five different temperatures in the range of 20–40 °C. The rate versus temperature data were used for the calculation of activation energies from the Arrhenius plot shown in the insets of Fig. 9(a) and (b). The Arrhenius activation energies were found to be 60.4 ± 3.1 kJ/mol and 54.4 ± 2.9 kJ/mol for the Ni@zeolite catalyzed hydrolysis of sodium borohydride and ammonia-borane, respectively. The obtained activation energies are smaller than the same that of obtained by using nickel powder (63 kJ/mol) [58], Ni-Co-B (62 kJ/mol) [59], catalysts in the hydrolysis of sodium borohydride and $Ni_{0.97}Pt_{0.03}$ hollow spheres (57 kJ/mol) [60], bulk nickel (70 kJ/mol) [60], Rh@zeolite (67 kJ/mol) [31] catalysts in the hydrolysis of ammonia-borane, but still larger than the values recorded for Ru(0) NPs (41 kJ/mol) [56], Ru@zeolite

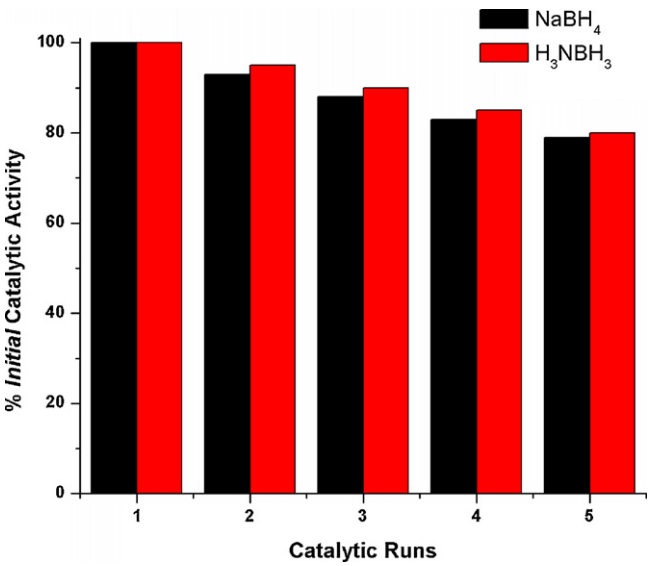

Fig. 10. The percentage of *initial* catalytic activity retained in the successive catalytic runs for Ni@zeolite catalyzed hydrolysis of sodium borohydride (black) and ammonia-borane (red), separately at $25.0 \pm 0.1\,^{\circ}C$. (For interpretation of the references to color in this figure legend, the reader is referred to the web version of the article.)

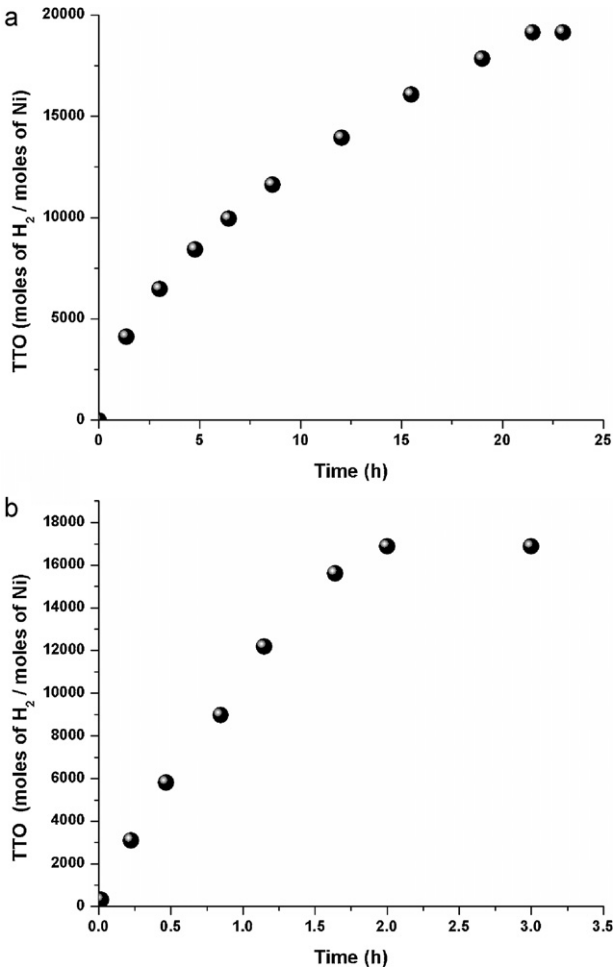

Fig. 11. Total turnover number (TTO) versus time plots for Ni@zeolite catalyzed hydrolysis of (a) sodium borohydride and (b) ammonia-borane at $25.0 \pm 0.1\,^{\circ}C$, starting with 50 mg Ni@zeolite (with a nickel content of 0.6 wt%).

(49 kJ/mol) [26] catalyzed hydrolysis of sodium borohydride and Ru(0) NPs (47 kJ/mol) [27], Rh(0) NPs (44 kJ/mol) [30] catalyzed hydrolysis of ammonia-borane.

3.6. Isolability and reusability of Ni@zeolite in the hydrolysis of sodium borohydride and ammonia-borane

Isolability and reusability of Ni@zeolite were also tested in the hydrolysis of both substrates. After the complete hydrolysis of 100 mM substrate solutions catalyzed by 4 mM Ni@zeolite at 25 °C, the catalyst was isolated as gray powders by suction filtration, washed with water, and dried under N_2 purging at room temperature. Gray samples of Ni@zeolite are bottled under nitrogen atmosphere. The ICP analysis did not show any nickel in the solution after filtration, indicating that there is no leaching of catalyst into the solution. The isolated Ni@zeolite are redispersible in water and yet show activity in the hydrolysis of sodium borohydride or ammonia-borane. Fig. 10 shows the changes in catalytic activity of Ni@zeolite in the hydrolysis of sodium borohydride and ammonia-borane with the number of catalytic runs at 25.0 ± 0.1 °C. It is noteworthy that Ni@zeolite retain 80% of their initial activity even at the fifth run in the hydrolysis of both substrates, ammonia-borane and sodium borohydride. This indicates that Ni@zeolite are isolable, bottleable, redispersible, and reusable. In other words, they can be repeatedly used as active catalyst in the hydrolysis of sodium borohydride or ammonia-borane. More importantly, the complete release of hydrogen is achieved in each of the successive catalytic runs. Since there is no leaching of nickel into the solution as determined by ICP, the slight decrease in catalytic activity in subsequent runs may be attributed to the passivation of nanoclusters surface by increasing the concentration of boron products, e.g. metaborate [61], which decreases accessibility of active sites [62] and the aggregation of nickel(0) nanoparticles as seen in the case of Rh(0)NPs@zeolite [31] and Cu(0)NPs@zeolite [38].

3.7. Catalytic lifetime of Ni@zeolite in the hydrolysis of sodium borohydride and ammonia-borane

The catalytic lifetime of Ni@zeolite in the hydrolytic dehydrogenations of sodium borohydride or ammonia-borane was determined by measuring the total turnover numbers they provided in both reactions. Fig. 11 shows the variations in total turnover number (TTO) versus time during the hydrolysis of sodium borohydride and ammonia-borane catalyzed by Ni@zeolite at 25.0 ± 0.1 °C. The zeolite confined nickel(0) nanoparticles provide 19,400 and 17,000 total turnovers in the hydrolysis of sodium borohydride and ammonia-borane, respectively, before deactivation.

4. Conclusions

In summary, our study of the preparation and characterization of Ni@zeolite catalyst for the hydrolytic dehydrogenations of sodium borohydride and ammonia borane have led to the following conclusions and insights:

(i) Ni@zeolite can easily be prepared at room temperature by ion-exchange of Ni^{2+} ions with the extra framework Na^+ ions in zeolite-Y, followed by reduction of the Ni^{2+} ions within the framework of zeolite-Y with sodium borohydride in aqueous solution at room temperature.
(ii) Ni@zeolite were found to be active catalyst in the hydrolysis of sodium borohydride and ammonia-borane even at low nickel concentration.
(iii) Moreover, the complete release of hydrogen is achieved even in each of successive runs performed by redispersing Ni@zeolite isolated after the previous run. Thus, Ni@zeolite are isolable, bottleable and redispersible. When redispersed in water, they retain essentially their initial catalytic activity with the complete hydrogen release in the hydrolysis of sodium borohydride or ammonia-borane.
(iv) Ni@zeolite are found to be long-lived catalyst as they provide 19,400 and 17,000 total turnovers in the hydrolytic dehydrogenations of sodium borohydride and ammonia-borane, respectively, at 25.0 ± 0.1 °C before they are deactivated.

Overall, Ni@zeolite are readily available by a simple and low cost procedure and are found to be highly active catalyst in the hydrogen generation from the hydrolysis of sodium borohydride and ammonia-borane. Therefore, it is worth to test them as catalyst in applications of hydrogen supply by using sodium borohydride or ammonia-borane as solid hydrogen storage material.

Acknowledgments

Partial support of this work by Turkish Academy of Sciences and TUBITAK (Project No: 105T366) is gratefully acknowledged.

References

[1] Basic Research Needs For the Hydrogen Economy, Report of the Basic Energy Sciences Workshop on Hydrogen Production, Storage and Use, Office of Science, U.S. Department of Energy, www.sc.doe.gov/bes/hydrogen.pdf May 13–15, 2003.
[2] Annual Energy Outlook 2005 With Projections To 2025, Energy Information Administration, www.eia.doe.gov/oiaf/aeo/pdf/0383(2005).pdf, February 2005.
[3] J. Turner, G. Sverdrup, K. Mann, P.G. Maness, B. Kroposki, M. Ghirardi, R.J. Evans, D. Blake, Int. J. Energy Res. 32 (2008) 379–407.
[4] IAC Report, Lighting the Way Towards a Sustainable Energy Futures, Interacademy Council, Amsterdam, 2007.
[5] P. Chen, Z.T. Xiong, J.Z. Luo, J.Y. Lin, K.L. Tan, Nature 420 (2002) 302–304.
[6] R. Bacsa, C. Laurent, R. Morishima, H. Suzuki, M. Lelay, J. Phys. Chem. B 108 (2004) 12718–12723.
[7] S.H. Lim, J. Luo, Z. Zhong, W. Ji, J. Lin, Inorg. Chem. 44 (2005) 4124–4126.
[8] J. Dong, X. Wang, H. Xu, Q. Zhao, J. Li, Int. J. Hydrogen Energy 32 (2007) 4998–5004.
[9] N.B. McKeown, P.M. Budd, Chem. Soc. Rev. 35 (2006) 675–683.
[10] J.A. Rood, B.C. Noll, K.W. Henderson, Inorg. Chem. 45 (2006) 5521–5528.
[11] M. Scheideman, G. Wang, E. Vedejs, J. Am. Chem. Soc. 130 (2008) 8669–8676.
[12] S.C. Amendola, J.M. Janjua, N.C. Spencer, M.T. Kelly, P.J. Petillo, S.L. Sharp-Goldman, M. Binder, Int. J. Hydrogen Energy 25 (2000) 969–975.
[13] M. Chandra, Q. Xu, J. Power Sources 156 (2006) 190–194.
[14] D. Wechsler, Y. Cui, D. Dean, B. Davis, P.G. Jessop, J. Am. Chem. Soc. 130 (2008) 17195–17203.
[15] C.W. Yoon, L.G. Sneddon, J. Am. Chem. Soc. 128 (2006) 13992–13993.
[16] Please see following excellent mini-review which briefly surveys the recent progresses in catalytic hydrolyses of metal hydrides and B-N compounds H.-L. Jiang, S.K. Singh, J.-M. Yan, X.-B. Zhang, Q. Xu, Chem. Sus. Chem. 3 (2010) 541–549.
[17] U.B. Demirci, P. Miele, Energy Environ. Sci. 2 (2009) 627–637.
[18] C.W. Hamilton, R.T. Baker, A. Staubitz, I. Manners, Chem. Soc. Rev. 38 (2009) 279–293.
[19] F.H. Stephens, V. Pons, R.T. Baker, Dalton Trans. 25 (2007) 2613–2626.
[20] E.Y. Marrero-Alfonso, A.M. Beaird, T.A. Davis, M.A. Matthews, Ind. Eng. Chem. Res. 48 (2009) 3703–3712.
[21] Q. Xu, M. Chandra, J. Power Sources 163 (2006) 364–370.
[22] J. Zhang, T.S. Fisher, J.P. Gore, D. Hazra, P.V. Ramachandran, Int. J. Hydrogen Energy 31 (2006) 2292–2298.
[23] M.E. Bluhm, M.G. Bradley, R. Butterick, U. Kusari, L.G. Sneddon, J. Am. Chem. Soc. 128 (2006) 7748–7749.
[24] A SciFinder literature search showed that in total >500 studies exist according to the terms "catalytic hydrolysis of sodium borohydride" and "catalytic hydrolysis of ammonia borane".
[25] M. Zahmakiran, S. Özkar, Langmuir 24 (2008) 7065–7067.
[26] M. Zahmakiran, S. Özkar, Langmuir 25 (2009) 2667–2678.
[27] F. Durap, M. Zahmakiran, S. Özkar, Int. J. Hydrogen Energy 34 (2009) 7223–7230.
[28] M. Chandra, Q. Xu, J. Power Sources 168 (2007) 135–142.
[29] T.J. Clark, G.R. Whittell, I. Manners, Inorg. Chem. 46 (2007) 7522–7527.
[30] F. Durap, M. Zahmakiran, S. Özkar, Appl. Catal. A: Gen. 369 (2009) 53–59.
[31] M. Zahmakiran, S. Özkar, Appl. Catal. B: Environ. 89 (2009) 104–110.
[32] M. Chandra, Q. Xu, J. Power Sources 159 (2006) 855–860.
[33] H.B. Dai, Y. Liang, P. Wang, H.M. Cheng, J. Power Sources 177 (2008) 17–23.
[34] M. Rakap, S. Özkar, Appl. Catal. B: Environ. 91 (2009) 21–29.

[35] Ö. Metin, V. Mazumder, S. Özkar, S. Sun, J. Am. Chem. Soc. 132 (2010) 1468–1469.
[36] H.-L. Jiang, T. Umegaki, T. Akita, X.-B. Zhang, M. Haruta, Q. Xu, Chem. Eur. J. 16 (2010) 3132–3137.
[37] Y. Li, L. Xie, Y. Li, J. Zheng, X. Li, Chem. Eur. J. 15 (2009) 8919.
[38] M. Zahmakiran, F. Durap, S. Özkar, Int. J. Hydrogen Energy 35 (2010) 187–197.
[39] M. Zahmakiran, S. Özkar, J. Mater. Chem. 19 (2009) 7112–7118.
[40] M. Zahmakiran, S. Özkar, Mater. Chem. Phys. 121 (2009) 359–363.
[41] M. Zahmakiran, S. Özkar, Mater. Lett. 63 (2009) 1033–1036.
[42] M. Zahmakiran, Y. Tonbul, S. Özkar, J. Am. Chem. Soc. 132 (2010) 6541–6549.
[43] D.W. Breck, Zeolite Molecular Sieves, Wiley, New-York, 1984.
[44] M. Zahmakiran, S. Özkar, Inorg. Chem. 48 (2009) 8955–8964.
[45] G. Guella, C. Zanchetta, B. Patton, A. Miotello, J. Phys. Chem. B 110 (2006) 17024–17033.
[46] S. Storck, H. Bretinger, W.F. Maier, Appl. Catal. A: Gen. 174 (1998) 137–146.
[47] R.S.H. Mikhail, S. Brunauer, E.E. Bodor, J. Colloid Interf. Sci. 26 (1968) 45–53.
[48] Handbook of X-ray Photoelectron Spectroscopy, vol. 55, Physical Electronic Division, Perkin-Elmer, 1979, p. 344.
[49] G. Schmid, Clusters and Colloids; From Theory to Applications, VCH Publishers, New York, 1994.
[50] L. Guczi, D. Bazin, Appl. Catal. A: Gen. 188 (1999) 163–174.
[51] Y.-X. Jiang, W.-Z. Weng, D. Si, S.-G. Sun, J. Phys. Chem. B 109 (2005) 7637–7642.
[52] A. Fukuoko, N. Higashimoto, Y. Sakamoto, S. Inagaki, Y. Fukushima, M. Ichikawa, Top. Catal. 18 (2002) 73–78.
[53] K. Okitsu, A. Yue, S. Tanabe, H. Matsumoto, Bull. Chem. Soc. Jpn. 75 (2002) 449–455.
[54] J.F. Xu, W. Ji, Z.X. Shen, W.S. Li, S.H. Tang, X.R. Ye, D.Z. Jia, X.Q. Xin, J. Raman Spectrosc. 30 (1999) 413–415.
[55] The self hydrolysis of ammonia-borane at room temperature does not take place as reported in literature (see Ref. [31]). However, the self hydrolysis of 150 mM sodium borohydride solution (in 50 mL) produces 94 mL H_2 gas over 2 h (see Ref. [50]).
[56] M. Zahmakiran, S. Özkar, J. Mol. Catal. A: Chem. 258 (2006) 95–103.
[57] The TOFs and TTOs reported herein are those typically reported [TOF = (mol of H_2 generated/mol of total catalyst loading × time]; [TTO = (TOF) × (time)]. That is, the reported TOFs and TTOs are not corrected for the amount of metal that is on the surface of the catalyst and/or the actual number of active sites.
[58] B.H. Liu, Z.P. Li, S. Suda, J. Alloys Compd. 415 (2006) 288–293.
[59] J.C. Ingersoll, N. Mani, J.C. Thenmozhiyal, A. Muthaiah, J. Power Sources 173 (2007) 450–457.
[60] S.B. Kalidindi, M. Indirani, B.R. Jagirdar, Inorg. Chem. 47 (2008) 7424–7429.
[61] XPS analysis of the recovered catalyst showed additionally a relatively weak boron 1s band at 187 eV indicating the existence of boron on the recovered catalyst.
[62] C.A. Jaska, T.J. Clark, S.B. Clendenning, D. Grozea, A. Turak, Z.-H. Lu, I. Manners, J. Am. Chem. Soc. 127 (2005) 5116–5124.